CONCRETE LIBRARY OF JSCE NO. 24, DECEMBER 1994

A STUDY ON THE ESTIMATION OF BENDING CRACK WIDTH ON THE SURFACES OF CONCRETE GIRDERS

(Translation from JSCE, Japan, No.484,V-22, 1994)

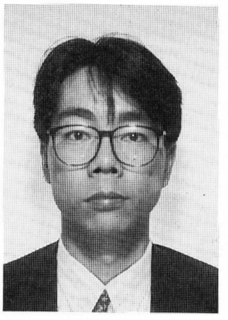

Tadayoshi ISHIBASHI　　Takeshi TSUYOSHI

SYNOPSIS

The width of cracks on the surface of concrete girders increases due to local drying shrinkage near the surface after initial cracking. Further, the stress in tensile reinforcement — the main factor affecting bending crack width — varies under the influence of drying shrinkage and creep. We examined a practical method of estimating reinforcement stress without considering concrete tensile stress as well as local drying shrinkage near the surface through experiments with reinforced concrete beams during drying. We also looked into measurements of bending crack width, spacing, and reinforcement stress in actual concrete girders for railways. This paper reports a practical method of calculating the bending crack width at the surface of concrete girders.

Keywords : concrete girder, surface, crack width, drying shrinkage

---

T. Ishibashi is a vice-director of the Tokyo Construction Office of East Japan Railway Company, Tokyo, Japan. He obtained his Doctor of Engineering degree from the University of Tokyo in 1984. His research interests include the seismic design of concrete structures for railways.

T. Tsuyoshi is an assistant-chief engineer in the structural engineering project team of the construction division of East Japan Railway Company. He graduated from the University of Tokyo in 1989. He engages in the design of reinforced concrete and prestressed concrete bridges for railways.

---

1. INTRODUCTION

Until now, serviceability of concrete structures for railways in the presence of bending cracks has been assured by a method in which the reinforcement stress during permanent loading is limited to within the allowable stress [1]. Meanwhile, the JSCE model code for concrete structures basically stipulates that the calculated value of maximum crack width be restricted within the limits defined for the serviceability limit state as determined by durability or external appearance. The precision with which estimates of bending crack width are made is critical to the design of structures where the serviceability limit state is verified in terms of bending crack width. Generally, while drying, the width of cracks on concrete surfaces increases as a result of local drying shrinkage [2]. Incidentally, in the JSCE model code, the design method for bending cracks relates mainly to the corrosion of reinforcement and prestressing strands, and local drying shrinkage is not clearly indicated as a method of estimating bending crack width. As matters now stand, however, the crack width where the surface is influenced by local drying shrinkage is one of indexes in practical use for maintaining actual structures. So a precise estimation and accurate restriction of the surface width for appearance can be said to be as important as the verification of steel corrosions.
We carried out experiments on reinforced concrete beams during drying and measured crack widths, spacings, and reinforcement stresses in order to increase the precision of estimates of surface bending crack width. We also derive a practical method for the precise estimation of bending crack width on concrete surfaces.

2. RESULTS OF EXPERIMENTS ON RC BEAMS [3][4]

To understand the influence of drying shrinkage on bending cracks, static bending experiments were carried out using reinforced concrete (RC) beams. The RC beams were maintained under fixed loading for about two years after initial cracking, and variations in bending crack width, crack spacing, and strain measurements using gages on reinforcement in the middle of the equivalent section of bending moment with time were measured.

Table 1 Specifications of Specimens

Specimen	Size(cm)	Reinforcement	Concrete age at initial cracking	Tensioning forces(kN)	Calculated tensile concrete stress * (MPa)
A − I	20×30× 230	Deform 19	14	38.2	7.64
A − II	20×30× 230	Deform 19	135		
B − I	20×30× 230	Deform 25	14	39.2	7.84
B − II	20×30× 230	Deform 25	135		

*) after loading (all section effective)

Note: Design Compressive Strength of Concrete $\sigma_{ck}=23.5$ (MPa)
Cement C=280(kg/m^3) Water W=154(kg/m^3)

Table 1 shows the specifications of specimens. Specimens were made in pairs with four-month spacings, so that the concrete age would be different at the time of initial cracking. The reinforced ratio was different in specimen A and specimen B. Fig. 1 shows the test equipment. Specimens I and II, which are of different ages, were combined, and by tensioning the prestressing bars positioned at both ends, a load was applied and bending cracks occurred. Specimens were then kept indoors and the prestressing forces managed using load cells to maintain a constant load. Specimens II were kept under drying conditions (indoors) after reaching the age of two weeks.

2. 1 Stresses in Reinforcement

Fig. 2 and Fig. 3 show the measured and calculated values of stresses in reinforcement with the passage of time. The calculations were carried out by considering strain conformity at the reinforcement position [3]. The assumptions made in the calculation are as follows.

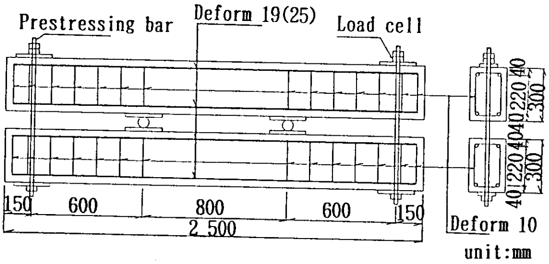

Fig. 1 Test Equipment

1. Forces in reinforcement against drying shrinkage are considered.
2. The condition of compatibility is applied.
3. Creep coefficient, drying shrinkage, and Young's modulus are calculated by Sakata's methods [5][6].
4. The relative humidity is 70%.

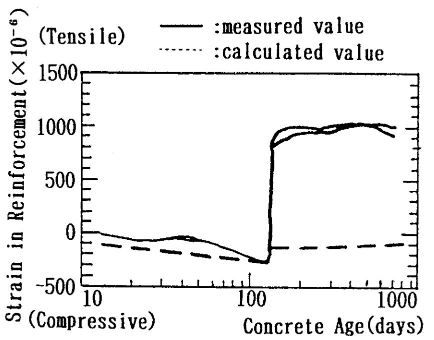

Fig. 2 Time-Variation of Strain in Reinforcement

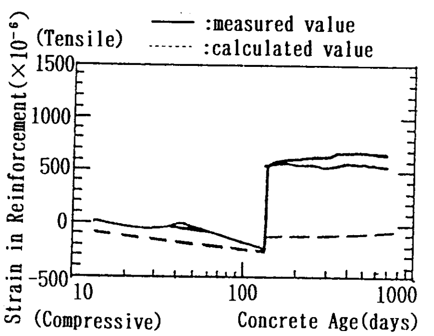

Fig. 3 Time-Variation of Strain in Reinforcement

After bending cracks occurred, calculated values and the measured values do not conform. This is expected because all concrete section are treated as effective with bending cracks ignored. But, until cracks occur, both values can be seen as conforming. So it can be said that the measured stresses in the reinforcement can be estimated relatively well by calculation before cracking.

Table 2 Stresses in Reinforcement in Crack Section

Specimen	Calculated value(MPa)	Measured value(MPa)	ϕ_{ci}	ε_{ci}
A − I	193.7	188.7	1.13	121
A − II	229.2	234.6	2.59	355
B − I	124.2	134.1	1.13	121
B − II	161.4	159.5	2.59	355

ϕ_{ci}:calculated value of creep coefficient before initial cracking
ε_{ci}:calculated value($\times 10^{-6}$) of drying shrinkage strain before initial cracking

Table 2 shows the calculated values [3] and measured values of tensile stresses in the reinforcement. The value represents the increase from the condition that the stress in concrete is zero at the position of the reinforcement. The assumptions made in this calculation are as follows.

1. Forces in reinforcement against drying shrinkage before initial cracking are considered.

2. Tensile stresses in concrete are ignored entirely.
3. The condition of compatibility can be applied.

Specimens Ⅱ which are older at loading have much larger drying shrinkage strain than specimens Ⅰ until bending cracks occurred. Larger axial compressive forces arise in the reinforcement of specimens Ⅱ. Thus, tensile stresses in reinforcement by cracking are larger in specimens Ⅱ than in specimens Ⅰ, and the measured values and calculated values are rather close.

After initial cracking, tensile stresses in the reinforcement vary with time lapse, mainly due to the influence of creep and drying shrinkage. However, the variations are not very large by calculation [7] and tne measured values are the same (Table 3). So, in the case of calculations of tensile stresses in the reinforcement at the crack section, as a practical design method, axial forces in the reinforcement against creep and drying shrinkage should be considered until bending cracks occur. Since the influences of creep and drying shrinkage to tensile stresses in reinforcements after cracking are relatively small.

Table 3 Time-Variations of Stresses in Reinforcement after Initial Cracking

Specimen	Measured value (MPa)	ϕ_{c2}	ε_{c2}
A − Ⅰ	4.8	2.52	312
A − Ⅱ	13.2	1.15	78
B − Ⅰ	-1.1	2.52	312
B − Ⅱ	9.9	1.15	78

ϕ_{c2}:calculated value of creep coefficient after initial cracking

ε_{c2}:calculated value of drying shrinkage strain($\times 10^{-6}$) after initial cracking

2. 2 Crack Width and Spacing

Fig. 4 shows bending cracks, directly after cracks occur. Table 4 shows the average measured values of crack widths and spacings immediately after initial cracking. Measurements of crack width are taken at the points of intersection with bending cracks and two standard lines made on the bottom surfaces of the specimens in the axial direction. Then cracks are examined in the equivalent section of bending moment without the fulcrum part. And because there are few measured points, and a qualitative tendency can be recognized clearly, crack widths and spacings are estimated by the average measured values.

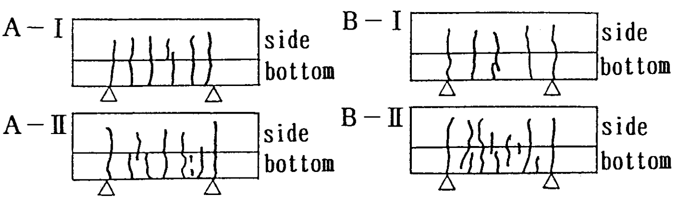

Fig. 4 Bending Crack Behavior

Specimens Ⅱ of greater age have smaller average crack spacings (Table 4). But, as mentioned in the section about average crack width directly after initial cracking, no distinctive qualitative tendency by age-difference can be seen.

Table 4 Measured Values of Crack Width and Spacing

Specimen	Average value of crack width (mm)	Average value of crack spacing (mm)
A − Ⅰ	146	0.09
A − Ⅱ	132	0.10
B − Ⅰ	164	0.10
B − Ⅱ	117	0.07

Table 5 shows the variations of crack width till 598 days after initial cracking. The average crack width increases much more rapidly for about 2 years. Generally, the crack width can be estimated as the product of crack spacing and strain discrepancy in the reinforcement and concrete between adjoining cracks as indicated by equation(1) [8].

$$w = \ell \cdot \Delta \varepsilon \tag{1}$$

where, ℓ : bending crack spacing
$\Delta\varepsilon$: strain discrepancy in reinforcement and concrete between adjoining cracks

Then, as for the strain discrepancy, the tensile stresses in the concrete between cracks are ignored, and it is estimated as the sum of reinforcement strains and the term related to drying shrinkage, which means the influence of local drying shrinkage near the crack surface (equation(2)).

$$\Delta\varepsilon = \sigma_{se}/E_s + \varepsilon_{SH} \qquad (2)$$

where,

σ_{se}/E_s : reinforcement strain

ε_{SH}: term related to drying shrinkage, meaning the influence of local drying shrinkage near the crack surface

Table 5 Time-Variation of Average Measured Values of Crack Width

t	Width (mm)	A−I	A−II	B−I	B−II
0	w_1	0.09	0.10	0.10	0.07
140	w_2	0.20	0.18	0.19	0.13
288	w_3	0.21	0.19	0.20	0.15
589	w_4	0.21	0.19	0.21	0.15
$\Delta w = w_4 - w_1$		0.13	0.09	0.11	0.08

t : Days after initial cracking

For each specimen, with the lapse of time, there is no variation in crack spacing. And the measured variation in tensile stresses in the reinforcements is not very large. Thus,it can be thought that the increase in crack width is caused mainly by local drying shrinkage near the crack surface. Table 6 shows the calculated values of ε_{sh} by equation(1) and (2).
The assumptions are indicated as follows.

1. As the values of w and ℓ, the measured values are adopted.
2. As the values of σ_{se}, the calculated value in the crack section is adopted.

Table 6 Calculated Values of ε'_{cs} ($\times 10^{-6}$)

	A−I	A−II	B−I	B−II
w(mm)	0.21	0.19	0.21	0.15
ℓ (mm)	146	132	164	117
ε_{SH}	517	348	675	491
ε_{SH}①	312	78	312	78
ε_{SH}②	446	214	441	217

w : Average measured crack width
ℓ : Average measured crack spasing
ε_{SH} : Calculated by equations (1) (2)
ε_{SH}①② : Calculated by Sakata's methods

Then, the calculated values of drying shrinkage strain in Table 6 by Sakata's method represent those after the age of initial cracking. To calculate the values ①, calculations were done on full-size specimens. And to calculate the values ②, calculations were done on small members divided by adjoinig bending cracks with one-fifth of the specimen's height [9]. Relative humidity is 70%. The values of ε_{sh} cannot be said to be caused only by local drying shrinkage, but they are much bigger than the calculated values ①, and they become relatively close to the calculated values ②. And the values by equations (1) and (2) are bigger in specimens I, where initial cracking occurs at younger age than in specimen II.

3. RESULTS OF MEASUREMENTS IN ACTUAL STRUCTURES

3. 1 Measurements in Actual Partially Prestressed Concrete Girders [10]

Table 7 shows the specifications of the partially prestressed girders for a railway on which measurements are carried out. In all girders, prestressing forces are introduced

Table 7 Specifications of Prestressed Reinforced Concrete Girders

Girder	Prestressing force (MN)	Mix proportion: Water content per unit (kg/m³)	Mix proportion: Cement content per unit (kg/m³)	Design compressive strength of concrete (MPa)	Covering (mm)	Spacing of reinforcement (mm)	Diameter of reinforcement (mm)	Span (m)
A	2.352	164	280	23.5	66	110	32	25.8
B 1	9.800	163	330	29.4	46	100	32	30.0
B 2	7.840	163	330	29.4	46	100	32	30.0
C 1	7.840	163	330	29.4	46	100	32	30.0
C 2	5.880	163	330	29.4	46	100	32	30.0

Table 8 Measured Values and Calculated Values

	Girder	A	B 1	B 2	C 1	C 2
Measured	Average crack width(mm)	0.11	0.05	0.07	0.05	0.05
	Average crack spacing(mm)	196	183	349	246	592
	Maximum crack width(mm)	0.25	0.15	0.25	0.15	0.20
	Crack spacing * (mm)	195	175	300	213	413
	Number of measured points	127	279	152	184	79
	Stresses in reinforcement (MPa)	35.0	68.6	102.7	45.7	70.2
Calculated	Maximum crack width(mm)	0.17	0.12	0.15	0.14	0.16
	Maximum crack spacing(mm)	319	232	232	232	232
	Stresses in reinforcement (MPa)	77.9	78.7	105.7	80.8	107.1
Concrete age at initial bending cracking		23	49	134	50	100

*) Average value of crack spacing adjacent to maximum crack width

only by external cables. They all have a cell-box section. The measurements were carried out two or three years after completion. The measured part is 3 meter long in the axial direction on the bottom surface at the middle of the span. And crack widths are measured using crack scales at the points of intersection between the bending cracks and standard lines in the axial direction, which are marked at 30 cm intervals on the bottom of the girders [11]. Then, the number and shape of bending cracks in these partially prestressed concrete girders look similar to the ones in general reinforced concrete girders.

Table 8 shows the measured values and calculated values of widths etc. The maximum measured crack width means that the measured points where measured values are over this width is less than

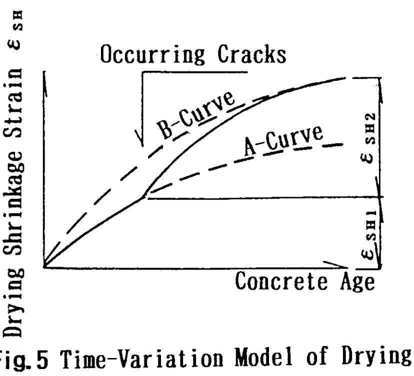

Fig.5 Time-Variation Model of Drying Shrinkage Strain after Cracking

5% in all measured points. (This is the definition of maximum measured crack width in this report.) Measured tensile stresses in the reinforcement are read from reinforcement strain gages at span centers.
The equation to calculate the maximum bending crack width is the following one (3) as prescribed in the JSCE model code. Conditions for calculations of tensile stresses in the reinforcement are as follows.

1. Calculations are carried out in the crack section during permanent loading.
2. Prestressing forces applied by external cables are treated as external forces.
3. Axial forces in reinforcement against creep and drying shrinkage until initial cracking are considered.
4. The age at which the initial crack occurs is the time at which supportings are withdrawn. The timing is judged from construction records (Table 8).
5. The value of ε'_{cs} is equal to 150×10^{-6} [12].

Then, at girder B1 and girder C1, prestressing strands are tensioned before withdrawing the supportings, and at girder B2 and girder C2, strands are tensioned after withdrawing the supportings.

$$w = k_1 \{4c + 0.7(c_s - \phi)\} \times (\sigma_{se}/E_s + \varepsilon'_{cs}) \qquad (3)$$

where, k_1 : a bond coefficient
c : covering
c_s : spacing of reinforcement
ϕ : diameter of reinforcement
σ_{se} : tensile stresses in reinforcement
E_s : Young's modulus of reinforcement
ε'_{cs} : strain for consideration to increase bending crack width by the influence of creep and drying shrinkage

The crack width is estimated as the product of the crack spacing and the strain discrepancy with concrete and reinforcement between adjoining bending cracks. So, to examine the precision of the equations for crack width, it is necessary to study these factors synthetic. But, as for bending surface crack widths under drying, the most influential factors of those causing errors in calculations of crack width can be expected to be the estimations of the influence of local drying shrinkage [10]. So, by focusing on an estimation of that, the following considerations are made.
From the results of experiments on RC beams, we can state that drying shrinkage strain, which increases the surface crack width, is much larger than the calculated strain values using the full-size of the specimens and that the strain is larger in the case of a younger age at which initial cracks occur. Then, to express these phenomena, we assume the time-variation curve for local drying shrinkage near crack surfaces shown in Fig. 5. That is to say, curve A shows the calculated values of drying shrinkage for a full-size specimen, and curve B shows those for a small member divided by adjoining bending cracks. We assume that the time-variation of local drying shrinkage near crack surfaces shifts from curve A to curve B when the initial crack occurs, and that ε_{sh2} shown in Fig. 5 is replaced by ε_{sh} in equation (2), representing the coefficient for the influence of local drying shrinkage which causes crack width to increase. This coefficient, proved clearly from Fig. 5, is bigger if the age at initial cracking is young, and so, the qualitative tendency found in the experiments by RC beams can be estimated.
Table 9 shows the calculated values of maximum crack width by this technique. The length in the axtial direction of divided members is equal to the calculated value of the term which shows the crack spacing in equation (3), and the height is the thickness of the under slab. The equations used to calculate drying shrinkage are those of Sakata's method [5], and relative humidity has two values, 60% and 70%.
In the case of 60% relative humidity, the calculated value is a little larger than the measured value, and good precision is obtained in the case of 70%. So, by the estimated method in which the influence of local drying shrinkage is expressed as mentioned in

Table 9 Calculated Values of Crack Width

Girder	A		B 1		B 2		C 1		C 2	
Relative humidity (%)	60	70	60	70	60	70	60	70	60	70
ε_{SH} ($\times 10^{-6}$)	454	368	430	368	353	324	417	356	359	321
σ_{SE} (MPa)	85.7	77.9	92.3	78.7	125	106	93.9	80.8	123	107
w_c (mm) :Calculated value	0.28	0.24	0.20	0.17	0.22	0.19	0.20	0.17	0.22	0.20
w_m (mm) :Measured value	0.25		0.15		0.25		0.15		0.20	
w_c / w_m	1.12	0.96	1.33	1.13	0.88	0.76	1.33	1.13	1.10	1.00

terms of the average strain of small members between cracks, the precision of the calculations of maximum bending crack width on a concrete surface is relatively good.

3.2 Measurements in Actual Reinforced Concrete Girders [13]

The specifications of the girders in which the measurements were carried out are shown in Table 10.

Table 10 Specifications of Reinforced Concrete Girders

Girder	Mix proportion: Water content per unit (kg/m³)	Mix proportion: Cement content per unit (kg/m³)	Design compressive strength of concrete (MPa)	covering (mm)	Spacing of reinforcement (mm)	ϕ (mm)	σ_{SE} (MPa)	Span (m)	N
D	166	325	23.5	66	80	32	126.9	19.1	17
E	166	325	23.5	66	84	32	103.9	14.1	6

σ_{SE}: Tensile stresses in reinforcement ϕ : Diameter of reinforcement

N : Numbers of measured girders

These girders were constructed at the same time and in the same location for Tohoku Shinkansen Bullet Train Line. The method of measuring bending cracks was the same as that for the partially prestressed concrete girders as mentioned before.
Fig. 6 and Fig. 7 show the distribution in bending crack widths, and Fig. 8 and Fig. 9 show the distribution of bending crack spacing.
The maximum measured spacing is compared with the calculated spacing by equation (3). The discrepancy between the measured value and the calculated value is within 5%, so it is recognized that the maximum crack spacing can be calculated precisely using equation (3).
Next, we compare the measured values and the calculated values of maximum bending crack width corresponding to each crack spacing. The method of estimating the influence of local drying shrinkage is the same as mentioned before, the humidity is 70%, and the height of small members divided by cracks is 30 cm for girder D, and 26 cm for girder E (representing one-fifth of the girder's height [9]). Initial cracking is assumed

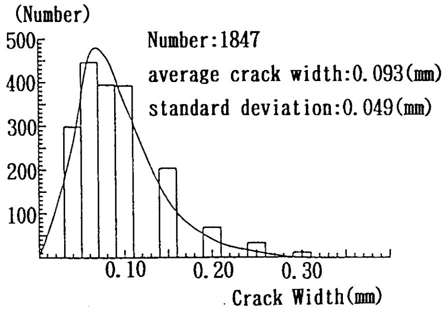

Fig.6 Distribution of Crack Width in Girder D

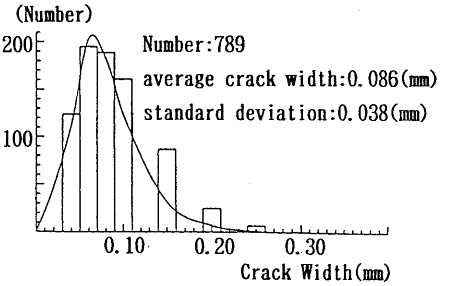

Fig.7 Distribution of Crack Width in Girder E

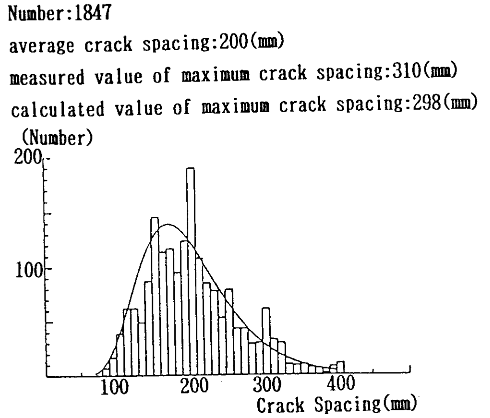

Fig.8 Distribution of Crack Spacing in Girder D

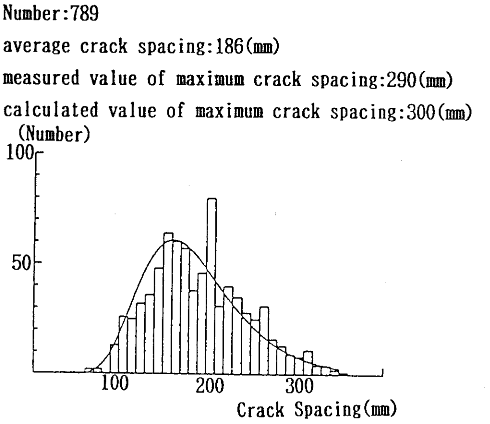

Fig.9 Distribution of Crack Spacing in Girder E

Table 11 Calculated Tensile Stresses in Concrete (MPa)

Girder	Own load	Permanent load	Design bending tensile strength
D	2.14	4.17	2.62
E	2.12	4.29	2.62

to occur after the total dead load is applied. This is judged from a comparison with the design bending tensile strength and with the calculated concrete tensile stresses as all concrete section are effective (Table 11). The timing of initial cracking is 100 days in consideration of an ordinary work schedule.
The calculated values 'ε_{sh2}' corresponding to each crack spacing - which are drying shrinkage as the small members divided by cracks - are shown in Table 12. The values are mostly within 300 to 400 $\times 10^{-6}$. A comparison with the measured values and calculated values of maximum bending crack width corresponding to each crack spacing are shown in

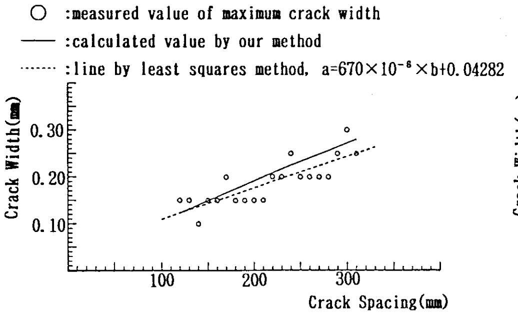

Fig. 10 Relationship between Crack Spacing and Crack Width in Girder D

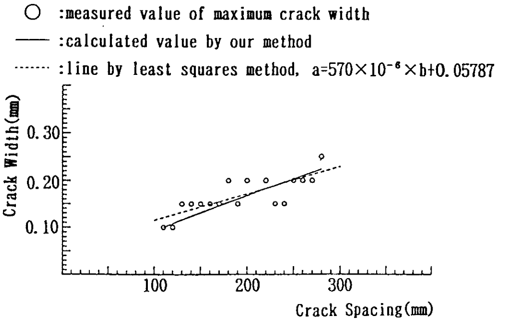

Fig. 11 Relationship between Crack Spacing and Crack Width in Girder E

Table 12 Calculated Values of ε'_{cs} ($\times 10^{-6}$)

Crack spacing (mm)	Girder D	Girder E	Crack spacing (mm)	Girder D	Girder E
100	426	415	210	336	328
110	415	405	220	330	322
120	405	395	230	324	317
130	395	386	240	319	312
140	386	377	250	314	307
150	378	368	260	309	302
160	370	361	270	304	297
170	362	354	280	299	293
180	355	347	290	295	289
190	348	340	300	291	285
200	342	334	———	———	———

Table 13 Discrepancies between Calculated and Measured Values of Maximum Crack Width

Girder	Our method		Least squares method	
	Dispersion (mm²)	Standard deviation (mm)	Dispersion (mm²)	Standard deviation (mm)
D	0.0011	0.0324	0.0007	0.0267
E	0.0006	0.0252	0.0005	0.0234

Fig. 10 and Fig. 11. In the calculations, the value of ε'_{cs} in equation (3) is applied as the one in Table 12, and the value of σ_{se} is calculated in the crack section during permanent loading.

On the other hand, from the results of measurements on other actual girders, Osaka et al. found out that the relationship between maximum bending crack width corresponding to each crack spacing and crack spacing can be estimated precisely by a one-dimensional correlation coefficient [14].

As for our measured results, similarly, a one-dimensional correlation is analyzed and shown in Fig. 10 and Fig. 11 by a dotted line. Table 13 shows the precision of calculations of maximum bending crack width. Table 13 indicates that the maximum bending crack width on the surface can be estimated relatively accurately by the method developed here.

Table 14 Specifications of Reinforced Concrete Girders

Girder	Type of section	Mix proportion: Water content per unit (kg/m^3)	Mix proportion: Cement content per unit (kg/m^3)	Design compressive strength of concrete (MPa)	σ_{SE1} (MPa)	σ_{SE2} (MPa)	ℓ (mm)	Span (m)
F	T	153	290	23.5	75.8	125.2	300	19.0
G	T	147	300	19.6	65.5	114.6	225	12.9
H	T	160	319	23.5	84.1	153.0	298	15.8
I	T	181	315	20.6	79.7	122.4	210	14.0
J	T	150	288	23.5	106.5	159.8	312	14.1
K	T	145	314	26.5	88.2	126.9	307	19.1
L	Box	145	314	26.5	129.6	178.9	307	24.1

σ_{SE1} : Tensile stresses during permanent load
σ_{SE2} : Tensile stresses during design load (permanent load + train load[EA-17] impact load)
ℓ : $4c + 0.7(c_s - \phi)$

Table 15 Calculated Values of Maximum Crack Width

	Girder F		Girder G		Girder H		Girder I		Girder J		Girder K		Girder L	
RH	60	70	60	70	60	70	60	70	60	70	60	70	60	70
ε	392	310	380	301	394	314	486	406	377	297	382	303	544	395
w_c	0.23	0.20	0.16	0.14	0.24	0.22	0.18	0.17	0.28	0.25	0.25	0.22	0.36	0.31
w_m	0.35		0.20		0.20		0.20		0.20		0.35		0.25	
R_c	0.86	0.57	0.80	0.70	1.20	1.10	0.90	0.85	1.40	1.25	0.71	0.63	1.44	1.24

RH : Relative humidity (%) ε : ε'_{SH2} ($\times 10^{-6}$)
w_c : Calculated value(mm) w_m : Measured value(mm)
R_c : w_c / w_m

Next, for actual bridges with the specifications shown in Table 14, a comparison between the measured values and calculated values of maximum bending crack width is carried out by our method. The results are shown in Table 15.
Initial crack is assumed to occur when an own dead laod is applied (this is the time when supportings are withdrawn). The time is assumed as 30 days for girder F－K, and 7 days for girder L, because travelling falsework is used for girder L. So, as mentioned before, the values of ε'_{cs} are calculated as drying shrinkage of small members divided by bending cracks, which proceed after cracking, and the maximum bending crack widths are calculated by equation (3). The relative humidity is 60% or 70%.
The value of drying shrinkage is influenced very much by the enviroment. So, in this case where the bridges are in different environments, a similar estimation of the environments (which is a estimation of the relative humidity) brings the large discrepancy between the measured and calculated values. But the average ratio of the measured and calculated values, in case of 70% of humidity, is 0.91, and 1.04 in 60%. And this seems to give a precise estimate of maximum bending crack width on the whole.

4. PROPOSED METHOD TO ESTIMATE THE MAXIMUM BENDING CRACK WIDTH ON SURFACES

4. 1 Method of Estimating the Maximum Bending Crack Width on Surfaces

As mentioned, we have recognized that the maximum bending crack width on the surface in an actual structure during permanent loading can be estimated relatively precisely. An equation to calculate the maximum bending crack width on surfaces is indicated as follows (equation (4)). This is based on the method in the JSCE model code [12].

$$w_2 = k_1 \{4c + 0.7(c_s - \phi)\} \times (\sigma_{se}/E_s + \varepsilon'_b) \qquad (4)$$

where,
- w_2 : maximum bending crack width on surface
- k_1 : a bond coefficient
- c : covering
- c_s : spacing of reinforcement
- ϕ : diameter of reinforcement
- σ_{se} : tensile stresses in reinforcement
- E_s : Young's modulus of reinforcement
- ε'_b : strain related to increase of bending crack width by the influence of local drying shrinkage near crack surface

The procedures and conditions for the calculation of σ_{se} are as follows.

1. to anticipate the cracking age by the comparison with the design tensile bending strength and the calculated tensile concrete stresses corresponding to work schedule
2. to consider axial forces in reinforcements caused by creep and drying shrinkage until the initial cracking for calculation of σ_{se}
3. to consider only permanent loads as the acting load

And the value of ε'_b is estimated as the drying shrinkage strain of small members divided by adjoining bending cracks, which proceed after initial cracking.

4. 2 The Value of ε'_b for Practical Design

Trial calculation is carried out to decide on a value of ε'_b for practical design. Concrete age at initial bending cracking is given as a parameter. As for the acting load, we consider three patterns; the girder's own load, the total dead load, and the design load including the train live load. For each load condition, by comparison with the design bending tensile strength and the calculated tensile concrete stresses, the cracking age is judged. The ages are 30, 100, and 200 days corresponding to each load condition. These are decided from an ordinary work schedule. This classification is adopted for normal concrete structures for railways as follows.

1. 30 days as the age of initial cracking is applied for reinforced concrete girders, beams in rigid frame structures.
2. 100 days is applied for partially prestressed concrete girders using external cables only. (Because the tensile concrete stresses against the girder's own load are restricted to within the design bending tensile strength in that structural type.)
3. 200 days is applied for partially prestressed concrete girders using bonded cables. (Because the tensile concrete stresses against the total dead load are restricted to within the design bending tensile strength in that structural type.)

Table 16 shows the value of ε'_b. The shrinkage strain is calculated by Sakata's method as the one of small members divided by cracks so as to involve the actual girder's condition of safety.
We believe that the value in Table 16 may be used in practical design.

5. CONCLUSION

5. 1 Experiments on RC Beams

1. Axtial forces in reinforcement before cracking caused by creep and drying shrinkage are estimated relatively accurately by the strain conformity at the reinforcement position.
2. The variation in stresses in reinforcements after cracking caused by creep and shrinkage are not very large.
3. In the case of calculations of tensile stresses in reinforcement at the crack section in consideration of axtial forces in reinforcement caused by creep and drying shrinkage, considering values before cracking is adequate for practical use as values of creep and drying shrinkage.
4. The crack width caused by local drying shrinkage near the concrete surface is rather large. And in a case where the increase in width is estimated by the average strain between adjoining bending cracks, it is much larger than the shrinkage strain calculated for full-size specimens. And the increase in width is larger if initial cracking occurs at younger age.

Table 16 Proposed Value of ε'_b ($\times 10^{-6}$)

Concrete age at initial cracking (day)	ε'_b
30	450
100	350
Morethan 200	300

5. 2 Measurement of Actual Girders

1. The crack spacing can be estimated precisely by the method given in the JSCE model code.
2. Strain discrepancy with concrete and reinforcements between adjoining bending cracks can be estimated as a sum of the tensile strain in reinforcements during permanent loading and drying shrinkage for small members divided by cracks.
3. As mentioned before, we propose a method for calculating the maximum bending crack width on a concrete surface during drying which uses as a parameter the concrete age at cracking.

REFFERENCES

[1] The Standard Code of Japan National Railway for Reinforced Concrete Structures and Plain Concrete Structures; JSCE,1983

[2] M. Yachida, T. Ishibashi, and T. Sato: Investigations and Studies about Bending Cracks and Steel Corrosions in Reinforced Concrete Bridges for Railway, JSCE, Feb., 1987

[3] T. Ishibashi, K. Saito, T. Tsuyoshi, M. Oba, and T. Suehiro: A Study on Influences of Concrete Age at Initial Cracking to Bending Crack Behaviors of Reinforced Concrete Beams, Journal of Structural Engineering, Vol. 37A, Mar., 1991

[4] T. Tsuyoshi, M. Oba, and T. Ishibashi: A Study on Time-Variation of Bending Crack Widths of Reinforced Concrete Beams, Proceedings of JCI, Vol. 14, No. 2, 1992

[5] K. Sakata and K. Ayano: Proposal of Predict Equations for Drying Shrinkage of Concrete, Extended Abstracts, the 43th Annual Meeting of JCA, 1989

[6] K. Ayano, S. Higai, Y. Onishi, and K. Sakata: A Study on Creep Property of Concrete with Variable Stresses, Proceedings of JCI, Vol. 12, No. 1, 1990

[7] Y. Kakuta: Calculation of Stresses in Crack Section and Control of Cracks, Concrete Journal, Vol. 25, No. 7, 1987

[8] Y. Kakuta: Maximum Crack Width in Reinforced Concrete Beams, Concrete Journal,Vol. 8, No. 9, Sep., 1970

[9] T. Tsuyoshi and T. Ishibashi: A Study on the Method to Estimate Maximum

Bending Crack Width, Extended Abstracts, the 45th Annual Meeting of JSCE, V-142, 1990
[10] T. Ishibashi, K. Tateishi, and T. Tsuyoshi: A Study on Crack Widths in Prestressed Reinforced Concrete Girders, Proceedings of JCI, Vol. 12, No. 2, 1990
[11] M. Oba, A. Yonai, K. Takeuchi, and T. Ishibashi: Investigations and Studies on Crack Bevaviors in Prestressed Reinforced Concrete Girders for Railway, Proceedings of JCI, Vol. 12, No. 2, 1989
[12] Model Code to Design Concrete Structures: JSCE, 1987 and 1991
[13] T. Ishibashi, K. Saito, and T. Tsuyoshi: Studies on Influences of Drying Shrinkage to Bending Crack Widths on Concrete Surfaces, Proceedings of JCI, Vol. 13, No. 1, 1991
[14] Y. Osaka, K. Otsuka, and H. Matsumoto: Tension Cracking Behavior of RC Beam Girders, JSCE, No. 390, Feb., 1988